HHS Public Access

Author manuscript

Oncogene. Author manuscript; available in PMC 2019 September 24.

Published in final edited form as:

Oncogene. 2008 December 04; 27(53): 6738–6748. doi:10.1038/onc.2008.265.

Cyclin D1 in low-dose radiation-induced adaptive resistance

KM Ahmed[1], **M Fan**[1], **D Nantajit**[1], **N Cao**[1], **JJ Li**[1,2]

[1]Division of Molecular Radiobiology and Graduate Program of Radiation and Cancer Biology, Purdue University School of Health Sciences, West Lafayette, IN, USA

[2]Purdue Cancer Center, West Lafayette, IN, USA

Abstract

Cyclin D1 is involved in cell-cycle arrest in DNA-damage response. This study tested the hypothesis that cyclin D1 regulates mitochondrial apoptosis. Cyclin D1 was induced by low-dose ionizing radiation (LDIR; 10-cGy X-ray) in human keratinocytes with an adaptive radioresistance that can be inhibited by short interfering RNA (siRNA)-mediated cyclin D1 inhibition. Cyclin D1 was found to form complex with chaperon 14-3-3ζ in unstressed cells and mutation of 14-3-3ζ Ser-58 to Asp (S58D) significantly impaired 14-3-3ζ binding to cyclin D1. The formation of cyclin D1/14-3-3ζ complex was differently regulated by exposure to low (10-cGy X-ray) versus high (5-Gy γ-ray) doses of radiation. Unlike exposure to 5-Gy that predominantly enhanced cyclin D1 nuclear accumulation, LDIR induced the dissociation of the cyclin D1/14-3-3ζ complex without nuclear translocation, indicating that cytosolic accumulation of cyclin D1 was required for LDIR-induced adaptive response. Further studies revealed a direct interaction of cyclin D1 with proapoptotic Bax and an improved mitochondrial membrane potential ($\Delta\psi_m$) in LDIR-treated cells. Consistently, blocking cyclin D1/Bax formation by cyclin D1 siRNA reversed $\Delta\psi_m$ and inhibited the LDIR-associated antiapoptotic response. These results demonstrate the evidence that cytosolic cyclin D1 is able to regulate apoptosis by interaction with Bax in LDIR-induced adaptive resistance.

Keywords

radiation resistance; cyclin D1; 14-3-3; Bax; human keratinocytes; adaptive response

Introduction

Mammalian cells exposed to certain low-dose ionizing radiation (LDIR) are evidenced to generate beneficial effects on maintenance of genomic integrity and the ability to repair damaged DNA (Kelsey *et al*, 1991; Feinendegen *et al*., 1996; Klokov *et al*., 2004). The adaptive radioresistance induced by LDIR is also demonstrated by an enhanced cell survival to subsequent high-dose ionizing radiation (HDIR) (Limoli *et al*., 2001; Ulsh *et al*., 2004). Although specific gene expression patterns have been linked with the altered cell radiosensitivity, the exact mechanisms governing the LDIR-associated advantage in cell

Correspondence: Dr JJ Li, Division of Molecular Radiobiology and Graduate Program of Radiation and Cancer Biology, Purdue University School of Health Sciences, 550 Stadium Mall Drive, West Lafayette, IN 47907, USA. jjli@purdue.edu.

survival remain elusive. Elucidating the molecular mechanisms of LDIR-induced radioresistance may provide mechanistic insights in radiation response and tumor radiosensitivity.

Mitochondria are key integrators of diverse metabolic signals, including production of reactive oxygen species. Aging and tumorigenesis are associated with mitochondrial DNA mutations and mitochondrial function is being considered as a potential target for cancer therapies (Costantini *et al.*, 2000). LDIR-induced adaptive response is linked with alterations of total mitochondrial protein translocation rate (Pandey *et al.*, 2006). NF-κB (nuclear factor-kappa B; a well-documented stress-responsive transcription factor) upregulates mitochondrial antioxidant manganese-containing superoxide dismutase in tumor necrosis factor-α-(Daosukho *et al.*, 2002) and ionizing radiation (IR)-treated cells (Guo *et al.*, 2003; Fan *et al.*, 2007). These results implicate an active role of mitochondrial apoptosis in signaling an adaptive resistance to mammalian cells. The mitochondrial antiapoptotic Bcl-2 and proapoptotic Bax are key factors for maintaining the mitochondrial membrane potential ($\Delta\psi_m$) and mitochondrial apoptosis (Karbowski *et al.*, 2006). Bcl-2 antagonizes the proapoptotic activity of Bax by direct forming Bcl-2/Bax heterodimers and the ratio of Bcl-2 to Bax is demonstrated to regulate the change of $\Delta\psi_m$ and apoptosis (Zhang *et al.*, 2000). Further evidence indicates that Bax activity is diminished in cells with elevated $\Delta\psi_m$ to prevent apoptosis. It is unknown, however, whether Bax-mediated $\Delta\psi_m$ alteration is involved in LDIR-induced radioadaptive response.

Cyclin D1 encodes a regulatory subunit of the holoenzyme that phosphorylates and inactivates the retinoblastoma protein to promote nuclear DNA synthesis (Sherr, 1994). Cyclin D1 is overexpressed in a variety of tumors (Oyama *et al.*, 1998) and is linked with tumor therapy resistance and a poor prognosis of cancer (Biliran *et al.*, 2005). Cyclin D1 is normally sequestered in the cytoplasm to reduce cell death, whereas apoptosis is induced when its nuclear localization is enforced (Sumrejkanchanakij *et al.*, 2003). In addition, 14-3-3 chaperons (14-3-3s) are shown to have critical role in DNA-damage-induced cell-cycle checkpoint control and cell survival by regulation of subcellular protein traffics (Xiao *et al.*, 1995). Inhibition of 14-3-3s sensitizes cancer cells to radiation (Qi and Martinez, 2003). The radioprotective function of 14-3-3s has been linked with the direct interaction and inhibition of proapoptotic Bax (Nomura *et al.*, 2003), sequestration of cytoplasmic c-Abl (Yoshida *et al.*, 2005) and relocation of apoptosis-promoting forkhead transcription factor FKHRL1 to cytoplasm (Brunet *et al.*, 1999).

Using LDIR (10-cGy X-ray)-irradiated human skin keratinocytes, the present study reveals a novel antiapoptotic function of cyclin D1 in LDIR-induced adaptive radiation resistance. A substantial amount of cyclin D1 was induced in human keratinocytes after exposure to LDIR, and the cytosolic cyclin D1 was predominantly induced in low rather than high-dose radiation, indicating that cyclin D1 is involved in mitochondrial apoptosis. Short interfering RNA (siRNA)-mediated cyclin D1 inhibition blocked cyclin D1/Bax interaction and eliminated LDIR-induced adaptive resistance. Thus, the accumulated cytosolic cyclin D1 proteins may have important role in inhibiting mitochondrial apoptosis in radiation-induced adaptive response.

Results

Cyclin D1 was induced in LDIR-mediated adaptive response

As cyclin D1 was highly expressed in the radio-resistant cells following long-term radiation (Guo *et al.*, 2003), we examined the potential role of this protein in LDIR-mediated adaptive radioresistance in immortalized human skin keratinocytes HK18. Long-term LDIR with 0.5-cGy per fraction per day substantially induced the expression of cyclin D1 (Figure 1a, upper panel). Two possible mechanisms are responsible for the increased cyclin D1 protein level: gene transcriptional activation and reduced cyclin D1 degradation. A single dose of 0.5-cGy was able to enhance cyclin D1 levels (Figure 1a, lower panel), indicating that each subsequent exposure may be additive to the previous exposure. A single exposure (10-cGy X-ray) remarkably induced cyclin D1 at 30 min that remained an elevated level 8 h after radiation (Figure 1b). In contrast, cyclin D1 induction was significantly delayed in HK18 cells exposed to HDIR (5-Gy γ-ray; Figure 1b), suggesting that different kinetics in cyclin D1 expression and protein degradation is induced by exposure to LDIR versus HDIR. A striking advantage of clonogenic survival of the LDIR-treated HK18 cells was detected when a challenge high dose of 5-Gy γ-ray was tested (Figure 1c).

To determine whether cyclin D1 is involved in the LDIR-induced adaptive radioresistance, cyclin D1 siRNA was applied in HK18 cells irradiated with the same sequence of low and high doses of radiation. Compared with scrambled siRNA control, LDIR-induced clonogenic radioresistance was absent in cyclin D1 siRNA-treated cells (Figure 1d). However, the siRNA treatment did not totally block the endogenous cyclin D1 (Figure 1d inset), indicating that LDIR-induced prosurvival pathways are sensitive to cyclin D1 protein level. Although the scrambled siRNA did show a toxicity that reduced cell-plating efficiency, treatment with scrambled and cyclin D1 siRNA did not induce difference in radiosensitivity in 5-Gy-treated cells, suggesting that a certain high level of cyclin D1 is specifically required for LDIR-induced adaptive resistance.

Subcellular distribution of cyclin D1 in LDIR- versus 5-Gy γ-ray-treated cells

Subcellular localization of cell-cycle proteins has been indicated to be important in determining cell radiosensitivity. Thus, we studied the levels of cyclin D1 in subcellular fractions after LDIR. Under long-term exposure of LDIR (0.5-cGy X-ray per fraction per day × 10), cyclin D1 was found to be predominantly accumulated in the cytoplasm but not in the nucleus (Figure 2a). To determine whether cyclin D1 subcellular distribution was differently regulated in low- and high-dose-irradiated cells, we detected cyclin D1 levels in the fraction of cytosolic and nuclear proteins of HK18 cells. Compared to the total cell lysate shown in Figure 1b, only a slight increase of cyclin D1 was detected in the cytoplasm of low radiation-treated cells (2 h compared to W; Figure 2b). However, there was no obvious increase of cyclin D1 detected in the cytoplasm of 5-Gy-irradiated cells (Figure 2b). In sharp contrast to high-dose radiation that induced significant nuclear translocation of cyclin D1, there was no nuclear cyclin D1 detected at 8h after 10-cGy radiation. Immunohisto-chemistry analysis of HK18 cells or mouse skin tissues further revealed that cyclin D1 nuclear translocation was predominantly enhanced by high but not low dose of radiation (Figures 2c and d). Thus, the sustained cyclin D1 protein level in cytoplasm of

LDIR-treated skin keratinocytes may be important in LDIR-induced adaptive radioresistance.

Dissociation of cyclin D1/14-3-3ζ complex in LDIR-treated cells

The 14-3-3 chaperon proteins function to subcellularly localize specific signaling element. As 14-3-3ζ-mediated protein translocation is demonstrated to have an important role in different cellular functions, we asked whether LDIR-induced cytoplasmic accumulation of cyclin D1 is mediated by 14-3-3ζ. Co-immunoprecipitation assay detected a novel interaction between cyclin D1 and 14-3-3ζ (Figure 3a). Interestingly, in contrast to 5-Gy γ-ray that induced little alteration of the cyclin D1/14-3-3ζ complex, the cyclin D1/14-3-3ζ interaction was significantly reduced by LDIR with an estimated decrease of ~ 50 times shown in Figure 3a (right panel). In consistence with LDIR-induced cyclin D1/14-3-3ζ dissociation (Figure 3b, upper panel), increased free cytoplasmic cyclin D1 was detected by western blot with the supernatant fraction of IP (Figure 3b). Figure 3c further demonstrates the cyclin D1/14-3-3ζ complex in the cytoplasm that was significantly reduced after LDIR. These results clearly indicate that LDIR dissociates the cyclin D1/14-3-3ζ complex, which together with the enhanced cyclin D1 protein expression by LDIR shown in Figures 1a and b, suggests that an increased cytoplasmic cyclin D1 accumulation is a predominant feature of LDIR-induced adaptive resistance.

To verify that 14-3-3ζ was required for cyclin D1 nuclear transport in HDIR-treated cells that show a preapoptotic response, HK18 cells were treated with siRNA against 14-3-3ζ before 5-Gy irradiation. HK18 cells incubated with 14-3-3ζ siRNA showed a significant inhibition of 14-3-3ζ expression (Figures 3d and e, upper panel). Consistently, treatment with 100 nM 14-3-3ζ siRNA, but not scramble siRNA, inhibited the nuclear translocation of cyclin D1 at 8 h post-5-Gy irradiation (Figures 3d and e, lower panel). Although siRNA-mediated 14-3-3ζ did not totally block the endogenous protein expression, radiation-induced nuclear translocation of cyclin D1 was totally blocked. This discrepancy suggests that a certain level of 14-3-3ζ protein is required for cyclin D1 nuclear translocation in high-dose radiation. Thus, the different response of cyclin D1/14-3-3ζ complex in low- and high-dose radiation represents a crucial evidence that 14-3-3ζ regulates cyclin D1 distribution, resulting in an increased level of cytoplasmic free cyclin D1 available for other cellular functions.

14-3-3ζ Ser-58 was required for interaction with cyclin D1

Powell *et al.* (2003) reported that mutation of 14-3-3ζ Ser-58 to Asp (S58D) significantly impaired interaction of 14-3-3ζ with Raf-1. Also, S58D inhibited the dimerization of 14-3-3ζ to dimerize. To determine whether Ser-58 of 14-3-3ζ is required for interaction with cyclin D1, we applied the bimolecular fluorescence complementation technique (Hu *et al.*, 2002) in living cells. HK18 cells were transfected with the fusion vectors encoding pFlag-14-3-3ζ-YN173 and pHA-cyclin D1-YC156, or pFlag-14-3-3ζ S58D-YN173 and pHA-cyclin D1-YC156 (schematic vectors are shown in the top of Figure 4a). Protein-protein interaction at 24 h after irradiation with 10-cGy X-ray was visualized under fluorescence microscopy. Interaction of 14-3-3ζ with cyclin D1 mostly in the cytoplasm was severely reduced when Ser-58 of 14-3-3ζ was mutated to Asp (Figure 4a). To verify the

requirement of Ser-58 for interaction of 14-3-3ζ with cyclin D1, co-immunoprecipitation was applied with the cell extracts of HK18 cells treated as in Figure 4a. Compared with pFlag-14-3-3ζ-YN173 + pHA-cyclin D1-YC156-transfected cells, cyclin D1/14-3-3ζ interaction was extremely reduced in cells transfected with pFlag-14-3-3ζ S58D-YN173 + pHA-cyclin D1-YC156. However, endogenous 14-3-3ζ/cyclin D1 interaction was not affected (Figure 4b). Together with Figure 4a, this result suggests that a specific amino acid (that is, Ser-58) of 14-3-3ζ is essential for interaction with cyclin D1 that is sensitive to radiation-induced stress.

Cyclin D1/Bax interaction in LDIR-induced $\Delta\psi_m$ alteration and adaptive radiation resistance

The expression levels of proapoptotic Bax and anti-apoptotic Bcl-2 proteins and their interaction are considered critical factors for maintaining $\Delta\psi_m$ and mitochondrial apoptosis. Figure 5a shows an increased Bax/Bcl-2 ratio (~ 28-fold) by 5-Gy radiation, which contrasted the low level of 0.74-fold alteration in 10-cGy X-ray-treated cells and 3.5-fold alteration in 10-cGy X-ray/5-Gy γ-ray-treated cells. Data of Figure 5b further revealed that cyclin D1 was able to interact with both Bcl-2 and Bax after low doses of radiation. However, the low radiation strikingly enhanced the cyclin D1/Bax interaction and reduced the Bcl-2/Bax interaction, which was opposite in 5-Gy-treated cells (Figure 5b, marked with a box). Furthermore, inhibition of cyclin D1 by siRNA eliminated the cyclin D1/Bax complex in 10-cGy-treated cells (Figure 5b, lower panel). Next, we determined whether cytoplasmic cyclin D1 accumulation is involved in the regulation of $\Delta\psi_m$, a key event in mitochondrial apoptosis. Figure 5c shows that release of mitochondrial cytochrome *c* to the cytosol, a result of damage in outer mitochondrial membrane, was significantly increased by 5-Gy IR than 10-cGy X-ray. Preexposure of 10-cGy also inhibited the 5-Gy-mediated cytochrome *c* release. Consistently, a significant decrease in $\Delta\psi_m$ was noticed in cells exposed to 5-Gy, whereas preexposure to LDIR almost totally reversed the loss of $\Delta\psi_m$ and the apoptotic response induced by 5-Gy alone (Figures 5d and e). Thus, the LDIR-induced $\Delta\psi_m$ protection and inhibition of apoptosis that can be eliminated by cyclin D1 siRNA suggest that maintaining a certain high level of cytoplasmic cyclin D1 is critical for LDIR-mediated adaptive radioresistance.

No alteration of cell cycle by HDIR with or without preexposure to LDIR

Mammalian cells exposed to a single HDIR activate cell-cycle checkpoints and cell-cycle arrest (Paulovich *et al.*, 1997). In light of our current results that cyclin D1, a key cell-cycle regulator for G_1/S-phase transition, is involved in mitochondrial apoptosis, it is logical to assume that LDIR-induced adaptive response is related with cyclin D1-mediated cell-cycle alteration. However, no significant difference was detected in the HK18 cells irradiated with 10-cGy/5-Gy radiation compared to 5-Gy alone (Table 1). These results are supportive to our finding that cyclin D1-mediated regulation of $\Delta\psi_m$ and mitochondrial apoptosis rather than cell-cycle regulation is required for LDIR-induced adaptive radioresistance.

Discussion

The present study demonstrates a novel mechanism of cyclin D1 in LDIR-mediated antiapoptotic response. In contrast to an HDIR (5-Gy γ-ray) that induced cyclin D1 nuclear translocation, LDIR (10-cGy X-ray) accumulated cyclin D1 in the cytoplasm and, interestingly, dissociated the cyclin D1/14-3-3ζ complex. The enhanced cytoplasmic cyclin D1 is confirmed to interact with and inhibit Bax with an improved $\Delta\psi_m$ in LDIR-induced adaptive radiation protection. Consistently, siRNA-mediated suppression of cyclin D1 inhibits cyclin D1/Bax complex formation with a reduced $\Delta\psi_m$ and eliminates LDIR-induced radioprotection. These results demonstrate that both cyclin D1 expression and cyclin D1/14-3-3ζ complex are able to enhance cytoplasmic cyclin D1 level, which maintains $\Delta\psi_m$ by direct interaction with Bax in adaptive radiation resistance.

The chaperon 14-3-3 proteins carry different cellular functions by binding and relocating their partners (Hermeking *et al.*, 1997), which are essential in regulation of cell-cycle checkpoints in DNA-damage response (Hermeking *et al.*, 1997; Yoshida *et al.*, 2005). The present study tested that ζ-isoform of 14-3-3 is involved in the subcellular distribution of cyclin D1 regulated in the LDIR-induced adaptive radioresistance. A novel complex formed by cyclin D1 and 14-3-3ζ is detected in resting human keratinocytes HK18 cells. Most interestingly, the response of this complex is strikingly different in low (10-cGy X-ray) versus high (5-Gy γ-ray) radiation. Mutational analysis revealed that Ser-58 of 14-3-3ζ is necessary for its interaction with cyclin D1. Compared with hDiR, cyclin D1/14-3-3ζ complex is significantly reduced after LDIR (Figure 3a), which causes the increase of free cyclin D1 in the cytoplasm (Figure 3b). Therefore, LDIR-induced cyclin D1 proteins shown in Figures 1a and b should contain a substantial amount of the free cyclin D1 dissociated from the cyclin D1/14-3-3ζ complex. Published results suggest a time of 4–6 h after low-dose radiation generates the maximal protection against the challenge of an HDIR (Shadley *et al.*, 1987). In agreement with the published data, in a previous study, we found that exposure of mouse skin epithelial cells to LDIR 6h before the high-dose challenge induced a significant level of adaptive response (Fan *et al*, 2007). This study on human skin epithelial cells also showed a significant induction of the adaptive radioresistance 6 h after exposure to 10-cGy (Figure 1c), suggesting a similar adaptive radioprotection between mouse and human skin cells. We also found that dissociation of cyclin D1/14-3-3ζ complex was enhanced at 8h after low-dose radiation. These results suggest the possibility that although cyclin D1 expression is induced, the free cyclin D1 dissociated from the cyclin D1/14-3-3ζ complex that occurs at late hours after radiation is responsible for the adaptive radioprotection. The complex cyclin D1/14-3-3ζ formed mainly in the cytoplasm (Figures 2a and b, and 3a) is confirmed by IP-western analysis (Figure 3c). The separation of cyclin D1 from 14-3-3ζ in LDIR-treated cells is apparently required for increasing the cytoplasmic retention of cyclin D1 that otherwise move to the nucleus under HDIR-induced cytotoxicity with a predominant apoptotic reaction. This is further supported by an obvious nuclear translocation of cyclin D1 by 14-3-3ζ in 5-Gy-treated cells (Figures 3d and e). The high dose-induced cyclin D1 nuclear translocation was further confirmed in the skin tissues of whole body-irradiated mice (Figure 2d), which was absent in low radiation-treated cells. These results reveal a specific 14-3-3ζ-mediated cyclin D1 subcellular translocation. The

exact mechanism underlying low and high radiation-induced cyclin D1/14-3-3ζ complex regulation is to be further investigated.

Sakamaki *et al.* (2006) reported that cytoplasmic sequestration of cyclin D1 is linked with altering $\Delta\psi_m$, a critical event in the control of apoptotic response and cell survival. In agreement with this report, the present study shows that a high dose of radiation (5-Gy γ-ray) decreased $\Delta\psi_m$ and released cytochrome *c* from mitochondria to the cytosol with induction of apoptosis (Figures 5c–e). However, unlike HDIR alone, preexposure to LDIR (10-cGy X-ray) prevents the high dose-induced loss of $\Delta\psi_m$ and apoptosis. Further study with siRNA indicates that inhibition of cyclin D1 blocks the LDIR-mediated protection of high dose-induced loss of $\Delta\psi_m$. Therefore, LDIR-induced accumulation of cytoplasmic cyclin D1 that can come from both enhanced protein expression and dissociation of the cyclin D1/14-3-3ζ complex has a key role for maintaining $\Delta\psi_m$ and the resistance to apoptosis by subsequent DNA damage induced by an HDIR.

It has been well-defined that Bcl-2 family of anti- and proapoptotic proteins regulates $\Delta\psi_m$ and mitochondrial apoptosis in radiation response (Yang *et al*, 1997; Karbowski *et al*, 2006). In this study, although the ratio of mitochondrial antiapoptotic Bcl-2 to proapoptotic Bax is increased in 5-Gy-treated cells, preexposure to LDIR significantly reverses the ratio (Figure 5a). Bcl-2 has been reported to directly interact with Bax (Sakamaki *et al*, 2006) to inhibit Bax-induced loss of $\Delta\psi_m$ and cytochrome *c* release. Importantly, as shown in Figure 5b, unlike exposure to 5-Gy IR that shows a lack of cyclin D1/Bax interaction, LDIR significantly enhances the interaction of cyclin D1 with Bax. Although 5-Gy-treated cells also demonstrate a slight enhancement of Bcl-2/Bax interaction that indicates a possible antiapoptotic response in high dose-irradiated cells, their levels were much less in LDIR-treated cells. Therefore, our current data strongly suggest that the free cytoplasmic cyclin D1 that can be enhanced by gene expression and dissociation from the cyclin D1/14-3-3ζ complex interacts and inhibits Bax to protect $\Delta\psi_m$ under the subsequent stress of HDIR. The distinct cyclin D1 subcellular localization and specific interaction with Bax may be crucial determinants for the different radiation sensitivity observed in mammalian cells.

It has been well-characterized that cell-cycle checkpoints and cell-cycle arrest are activated by a single HDIR (Paulovich *et al.*, 1997). It is reasonable to assume that LDIR induces a similar cell-cycle arrest as cyclin D1 is induced as shown in the present study. The common targets of LDIR and HDIR, for example, double (DSBs)- or single-strand breaks (SSBs), are a key threat to the integrity and stability of the genome. Understanding the fate of irradiated cells is primarily based on studies under conditions of lethal dose of IR. Reports further demonstrate that ~3% of low dose (10-cGy)-irradiated cells sustain DSBs and other forms of DNA damages that require cell-cycle regulation and DNA repair (Rothkamm and Lobrich, 2003). The exact role underlying the LDIR-induced DSBs or SSBs in inducing cell-cycle arrest and adaptive radioresistance is not clear. On the basis of these results, we analysed cell-cycle distribution of HK18 cells after radiation with sham, 10-cGy, 5-Gy or 10-cGy + 5-Gy. No significant difference was induced in the cell-cycle arrest between 5-Gy and 10-cGy + 5-Gy (Table 1). These results clearly demonstrate that cyclin D1-mediated regulation on mitochondrial apoptosis rather than the cell-cycle status is a determinant factor in LDIR-induced adaptive radioresistance.

In summary, the present data reveal a new function of cyclin D1 in LDIR-induced adaptive radioprotection. In contrast to the HDIR (5-Gy γ-ray) that induces 14-3-3ζ-dependent cyclin D1 nuclear import, LDIR (10-cGy X-ray) causes a dissociation of cyclin D1/14-3-3ζ complex that together with cyclin D1 protein expression increases the cyclin D1 accumulation in the cytoplasm. The free cyclin D1 protects the sequential insult of HDIR that otherwise enhances the loss of $\Delta\psi_m$ and apoptosis by binding to and suppressing proapoptotic Bax. Thus, cytoplasmic cyclin D1 accumulation represents a new therapeutic approach in adjustment of cell radiosensitivity.

Materials and methods

Cell culture and IR exposure

Human skin keratinocytes HK18 (Chen *et al.*, 2002) were maintained in Dulbecco's minimum Essential medium supplemented with 10% fetal bovine serum (HyClone, Logan, UT, USA), penicillin (100 units per ml) and streptomycin (100 mg/ml) in a humidified incubator (5% CO_2). For the long-term radiation with low-dose X-rays, exponentially growing HK18 cells in T25 flask with 70–80% confluence were exposed to radiation at room temperature using a Cabinet X-ray System Faxitron Series (dose rate: 0.028 Gy/min; Hewlett Packard, McMinnville, OR, USA). HDIR was delivered with the GR-12 irradiator equipped with a cobalt-60 (dose rate: 2.3 Gy/min; US Nuclear Corp., Burbank, CA, USA). Cells sheltered from low or high doses of radiation were used as the sham-IR control. The fractionated low dose-treated or sham-irradiated HK18 cells were maintained in complete medium and passaged every 3 days during the course of LDIR treatment. The cell growth status of 0.5-cGy-irradiated cells at different fractions was detected and no difference was measured compared to the sham-LDIR-treated cells. Radiation sensitivity was measured by clonogenic survival assay and apoptosis (Wang *et al.*, 2005).

Western blotting and immunoprecipitation

Immunoblotting was followed with the described methods (Wang *et al.*, 2005). The antibody preparations against 14-3-3ζ (sc-1019), actin (sc-8432), cyclin D1 (sc-20044), cytochrome *c* (sc-13560), Bax (sc-493) and Bcl-2 (sc-509) were purchased from Santa Cruz Biotechnology Inc., (Santa Cruz, CA, USA). Anti-Cox IV (ab14744) and -histone H3 (ab1791) were bought from Abcam (Canbridge, MA, USA). The antibodies of CuZuSOD (catalog no. 556360) and α-tubulin (T 6074) were obtained from BD Biosciences Pharmingen (Franklin Lakes, NJ, USA) and Sigma (St Louis, MO, USA), respectively. Immunoprecipitation was performed as previously described (Ahmed *et al.*, 2006).

Preparation of cytoplasmic and nuclear extracts

Cells were rinsed with phosphate-buffered saline (PBS) containing 1 mM EDTA, collected by centrifugation and resuspended in ice-cold hypotonic lysis buffer supplemented with protease inhibitors (10 mM 4-(2-hydroxyethyl)-1-piperazineethanesulfonic acid (HEPES), pH 7.9, 0.1 mM EDTA, 0.1 mM ethylene glycol tetraacetic acid (EGTA), 10mM KCl, 0.3% nonidet P-40 (NP-40), 1 mM dithiothreitol, 1 mM phenylmethylsulfonylfluoride (PMSF), 1 mg/ml leupeptin and 1 mg/ml pepstatin A). Following 15min of incubation on ice, the cell lysates were vortexed and centrifuged at 15 000 *g* for 1 min to obtain the nuclear pellet and

the cytosolic protein-containing supernatant. The nuclear pellets were washed using the aforementioned buffer with the exclusion of NP-40. Then the nuclei were resuspended in the ice-cold solution (20 mM HEPES, pH 7.9, 420 mM NaCl, 1mM EDTA, 0.1 mM EGTA, 1mM PMSF, 1 μg/ml leupeptin and 1 μg/ml pepstatin A). After 30 min of incubation on ice, the samples were centrifuged at 15 000 *g* for 5 min and the resulting supernatant was saved as nuclear extracts and stored in the −80 °C freezer until use for western analysis.

Silencing 14-3-3ζ and cyclin D1 expression by siRNA

siRNA capable of targeting mRNAs encoding 14-3-3ζ or cyclin D1 were synthesized with the Silencer siRNA Construction Kit (Ambion, Austin, TX, USA). The primers used to synthesize the siRNAs were as follows: AAACATCATTGCAGATATCTCCCTGTCTC (sense; 14-3-3ζ and AAGAGATATCTGCAATGATGTCCTGTCTC (antisense; 14-3-3ζ; AACAACTTCCTGTCCTACTACCCTGTCTC (sense; cyclin D1) and AAGTAGTAGGACAGGAAGTTGCCTGTCTC (antisense; cyclin D1). Cells were seeded to achieve 30–50% confluence and transfection of siRNA was performed using Lipofectamine RNAiMAX reagent (Invitrogen, Carlsbad, CA, USA) in 35mm plates with antibiotics-free medium for 24h before transfection with indicated amounts of siRNAs. Scramble RNA Duplex (Ambion) was included as control. Inhibition of 14-3-3ζ or cyclin D1 was determined by western blotting at 60 h post-transfection. All transfectants were maintained in antibiotics-free complete medium until collection for analysis.

Immunostaining and immunohistochemical analyses

HK18 cells transfected with 14-3-3ζ siRNA or scramble for 60 h and mouse tissue sections were examined by standard immunostaining and immunohistochemical protocols, respectively. For immunostaining, cells were irradiated with different doses and then fixed in ice-cold 3.7% formaldehyde followed by permeabilization in ice-cold 0.2% Triton X-100 for 5min, incubation with primary antibody (anti-cyclin D1 or anti-14-3-3ζ for 1 h and with the secondary antibody conjugated with Texas Red (Jackson ImmunoResearch Laboratories, West Grove, PA, USA) for 1 h. For immunohistochemical analysis, formalin-fixed, paraffin-embedded tissue sections (5 μM) were prepared from mice 24 h after whole-body irradiation with sham, 10-cGy X-ray or 5-Gy γ-ray. Following deparaffinization in xylene and rehydration through graded ethanol, the sections were incubated with primary antibody (anti-cyclin D1) for 1 h, followed by three washes, and the incubation with the secondary antibody conjugated with Texas Red for 1 h.

Imaging protein interactions in living cells

Full-length sequences encoding human 14-3-3ζ and 14-3-3ζ S58D, and cyclin D1 were fused to N- (residues 1–173) and C-terminal (residues 156–238), respectively, fragments of enhanced yellow fluorescent protein (EYFP). The coding region of 14-3-3ζ or 14-3-3ζ S58D, or cyclin D1 was connected with the coding region of N- or C-terminal of EYFP by linker sequences as previously described (Hu *et al.*, 2002). All the fusion constructs were confirmed by sequencing. HK18 cells growing in 96-well plates were co-transfected with 0.1 μg of each expression vector, that is, pFlag-14-3-3ζ-YN173 and pHA-cyclin D1-YC156 or pFlag-CMV-14-3-3ζ S58D-YN173 and pHA-cyclin D1-YC156, using Lipofectamine2000 (Invitrogen). The fluorescence emissions were observed in living cells

between 24 h after irradiation with 10-cGy using a Nikon TE300 inverted fluorescence microscope with a cooled CCD camera.

Assay of mitochondrial membrane potential

Cellular $\Delta\psi_m$ was determined using a fluorescent cationic dye, 5,5′,6,6′-tetrachloro-1,1′, 3,3′-tetraethyl-benzamidazolocarbo-cyanin iodide (JC-1; Molecular Probes, Eugene, OR, USA). The changes in $\Delta\psi_m$ were measured with the levels of relative fluorescence units, using a SpectraMax M5 MultiMode Microplate Reader (Molecular Devices, Sunnyvale, CA, USA), with a 485 nm excitation filter and a 525–595 nm emission filter.

Apoptosis assay

To detect apoptotic cells, terminal deoxynucleotidyltransfer-ase-mediated UTP end-labeling (TUNEL) method was used according to the manufacturer's instructions (ApopTag plus peroxidase *in situ* apoptosis detection kit (Chemicon, Temecula, CA, USA).

Flow cytometry analysis

Exponentially growing HK18 cells were exposed to sham-IR, 5-Gy γ-ray and 10-cGy X-ray with or without 6h postexposure to 5-Gy. At 24 h post-5-Gy-radiation, cells were trypsinized, counted and 1×10^6 cells were suspended in PBS containing 0.2mg/ml RNase, 0.1 mg/ml bovine serum albumin, 0.05mg/ml propidium iodide and 0.1% Triton X-100, and incubated for 30 min at room temperature. To determine the distribution of cells in G_1, S and G_2 phases, 2×10^4 cells were analysed by flow cytometry and the data were processed using IDLYK software (created at Los Alamos National Laboratory).

Acknowledgements

We thank Dr N Colburn (National Cancer Institute, NIH) for providing human keratinocytes HK18 cells, Dr S Liu (Purdue University School of Health Sciences) for invaluable help with animal experiments. This work was supported by NIH NCI grant RO1 101990 and the Department of Energy grant DE-FG02-03ER63634 to JJL.

Abbreviations

$\Delta\psi_m$	mitochondrial membrane potential
DAPI	4,6-diamidino-2-phenylindole
EYFP	enhanced yellow fluorescent protein
HDIR	high-dose ionizing radiation
IHC	immunohistochemistry
IR	ionizing radiation
LDIR	low-dose ionizing radiation
NP-40	nonidet P-40
PMSF	phenylmethylsulfonylfluoride

siRNA short interfering RNA

References

Ahmed KM, Dong S, Fan M, Li JJ. (2006). Nuclear factor κB P65 inhibits mitogen-activated protein kinase signaling pathway in radioresistant breast cancer cells. Mol Cancer Res 4: 945–955. [PubMed: 17189385]

Biliran H Jr, Wang Y, Banerjee S, Xu H, Heng H, Thakur A et al. (2005). Overexpression of cyclin D1 promotes tumor cell growth and confers resistance to cisplatin-mediated apoptosis in an elastase-myc transgene-expressing pancreatic tumor cell line. Clin Cancer Res 11: 6075–6086. [PubMed: 16115953]

Brunet A, Bonni A, Zigmond MJ, Lin MZ, Juo P, Hu LS et al. (1999). Akt promotes cell survival by phosphorylating and inhibiting a Forkhead transcription factor. Cell 96: 857–868. [PubMed: 10102273]

Chen X, Shen B, Xia L, Khaletzkiy A, Chu D, Wong JY et al. (2002). Activation of nuclear factor kappaB in radioresistance of TP53-inactive human keratinocytes. Cancer Res 62: 1213–1221. [PubMed: 11861406]

Costantini P, Jacotot E, Decaudin D, Kroemer G. (2000). Mitochondrion as a novel target of anticancer chemotherapy. J Natl Cancer Inst 92: 1042–1053. [PubMed: 10880547]

Daosukho C, Kiningham K, Kasarskis EJ, Ittarat W, St Clair DK. (2002). Tamoxifen enhancement of TNF-alpha induced MnSOD expression: modulation of NF-kappaB dimerization. Oncogene 21: 3603–3610. [PubMed: 12032862]

Fan M, Ahmed KM, Coleman MC, Spitz DR, Li JJ. (2007). Nuclear factor-kappaB and manganese superoxide dismutase mediate adaptive radioresistance in low-dose irradiated mouse skin epithelial cells. Cancer Res 67: 3220–3228. [PubMed: 17409430]

Feinendegen LE, Bond VP, Sondhaus CA, Muehlensiepen H. (1996). Radiation effects induced by low doses in complex tissue and their relation to cellular adaptive responses. Mutat Res 358: 199–205. [PubMed: 8946025]

Guo G, Yan-Sanders Y, Lyn-Cook BD, Wang T, Tamae D, Ogi J et al. (2003). Manganese superoxide dismutase-mediated gene expression in radiation-induced adaptive responses. Mol Cell Biol 23: 2362–2378. [PubMed: 12640121]

Hermeking H, Lengauer C, Polyak K, He TC, Zhang L, Thiagalingam S et al. (1997). 14-3-3 Sigma is a p53-regulated inhibitor of G_2/M progression. Mol Cell 1: 3–11. [PubMed: 9659898]

Hu CD, Chinenov Y, Kerppola TK. (2002). Visualization of interactions among bZIP and Rel family proteins in living cells using bimolecular fluorescence complementation. Mol Cell 9: 789–798. [PubMed: 11983170]

Karbowski M, Norris KL, Cleland MM, Jeong SY, Youle RJ. (2006). Role of Bax and Bak in mitochondrial morphogenesis. Nature 443: 658–662. [PubMed: 17035996]

Kelsey KT, Memisoglu A, Frenkel D, Liber HL. (1991). Human lymphocytes exposed to low doses of X-rays are less susceptible to radiation-induced mutagenesis. Mutat Res 263: 197–201. [PubMed: 1861683]

Klokov D, Criswell T, Leskov KS, Araki S, Mayo L, Boothman DA. (2004). IR-inducible clusterin gene expression: a protein with potential roles in ionizing radiation-induced adaptive responses, genomic instability, and bystander effects. Mutat Res 568: 97–110. [PubMed: 15530543]

Limoli CL, Kaplan MI, Giedzinski E, Morgan WF. (2001). Attenuation of radiation-induced genomic instability by free radical scavengers and cellular proliferation. Free Radic Biol Med 31: 10–19. [PubMed: 11425485]

Nomura M, Shimizu S, Sugiyama T, Narita M, Ito T, Matsuda H et al. (2003). 14-3-3 Interacts directly with and negatively regulates pro-apoptotic Bax. J Biol Chem 278: 2058–2065. [PubMed: 12426317]

Oyama T, Kashiwabara K, Yoshimoto K, Arnold A, Koerner F. (1998). Frequent overexpression of the cyclin D1 oncogene in invasive lobular carcinoma of the breast. Cancer Res 58: 2876–2880. [PubMed: 9661905]

Pandey BN, Gordon DM, De Toledo SM, Pain D, Azzam EI. (2006). Normal human fibroblasts exposed to high- or low-dose ionizing radiation: differential effects on mitochondrial protein import and membrane potential. Antioxid Redox Signal 8: 1253–1261. [PubMed: 16910773]

Paulovich AG, Toczyski DP, Hartwell LH. (1997). When checkpoints fail. Cell 88: 315–321. [PubMed: 9039258]

Powell DW, Rane MJ, Joughin BA, Kalmukova R, Hong JH, Tidor B et al. (2003). Proteomic identification of 14-3-3zeta as a mitogen-activated protein kinase-activated protein kinase 2 substrate: role in dimer formation and ligand binding. Mol Cell Biol 23: 5376–5387. [PubMed: 12861023]

Qi W, Martinez JD. (2003). Reduction of 14-3-3 proteins correlates with increased sensitivity to killing of human lung cancer cells by ionizing radiation. Radiat Res 160: 217–223. [PubMed: 12859233]

Rothkamm K, Lobrich M. (2003). Evidence for a lack of DNA double-strand break repair in human cells exposed to very low X-ray doses. Proc Natl Acad Sci USA 100: 5057–5062. [PubMed: 12679524]

Sakamaki T, Casimiro MC, Ju X, Quong AA, Katiyar S, Liu M et al. (2006). Cyclin D1 determines mitochondrial function *in vivo*. Mol Cell Biol 26: 5449–5469. [PubMed: 16809779]

Shadley JD, Afzal V, Wolff S. (1987). Characterization of the adaptive response to ionizing radiation induced by low doses of X rays to human lymphocytes. Radiat Res 111: 511–517. [PubMed: 3659285]

Sherr CJ. (1994). G_1 phase progression: cycling on cue. Cell 79: 551–555. [PubMed: 7954821]

Sumrejkanchanakij P, Tamamori-Adachi M, Matsunaga Y, Eto K, Ikeda MA. (2003). Role of cyclin D1 cytoplasmic sequestration in the survival of postmitotic neurons. Oncogene 22: 8723–8730. [PubMed: 14647467]

Ulsh BA, Miller SM, Mallory FF, Mitchel RE, Morrison DP, Boreham DR. (2004). Cytogenetic dose-response and adaptive response in cells of ungulate species exposed to ionizing radiation. J Environ Radioact 74: 73–81. [PubMed: 15063537]

Wang T, Hu YC, Dong S, Fan M, Tamae D, Ozeki M et al. (2005). Co-activation of ERK, NF-kappaB, and GADD45beta in response to ionizing radiation. J Biol Chem 280: 12593–12601. [PubMed: 15642734]

Xiao B, Smerdon SJ, Jones DH, Dodson GG, Soneji Y, Aitken A et al. (1995). Structure of a 14-3-3 protein and implications for coordination of multiple signalling pathways. Nature 376: 188–191. [PubMed: 7603573]

Yang J, Liu X, Bhalla K, Kim CN, Ibrado AM, Cai J et al. (1997). Prevention of apoptosis by Bcl-2: release of cytochrome *c* from mitochondria blocked. Science 275: 1129–1132. [PubMed: 9027314]

Yoshida K, Yamaguchi T, Natsume T, Kufe D, Miki Y. (2005). JNK phosphorylation of 14-3-3 proteins regulates nuclear targeting of c-Abl in the apoptotic response to DNA damage. Nat Cell Biol 7: 278–285. [PubMed: 15696159]

Zhang L, Yu J, Park BH, Kinzler KW, Vogelstein B. (2000). Role of BAX in the apoptotic response to anticancer agents. Science 290: 989–992. [PubMed: 11062132]

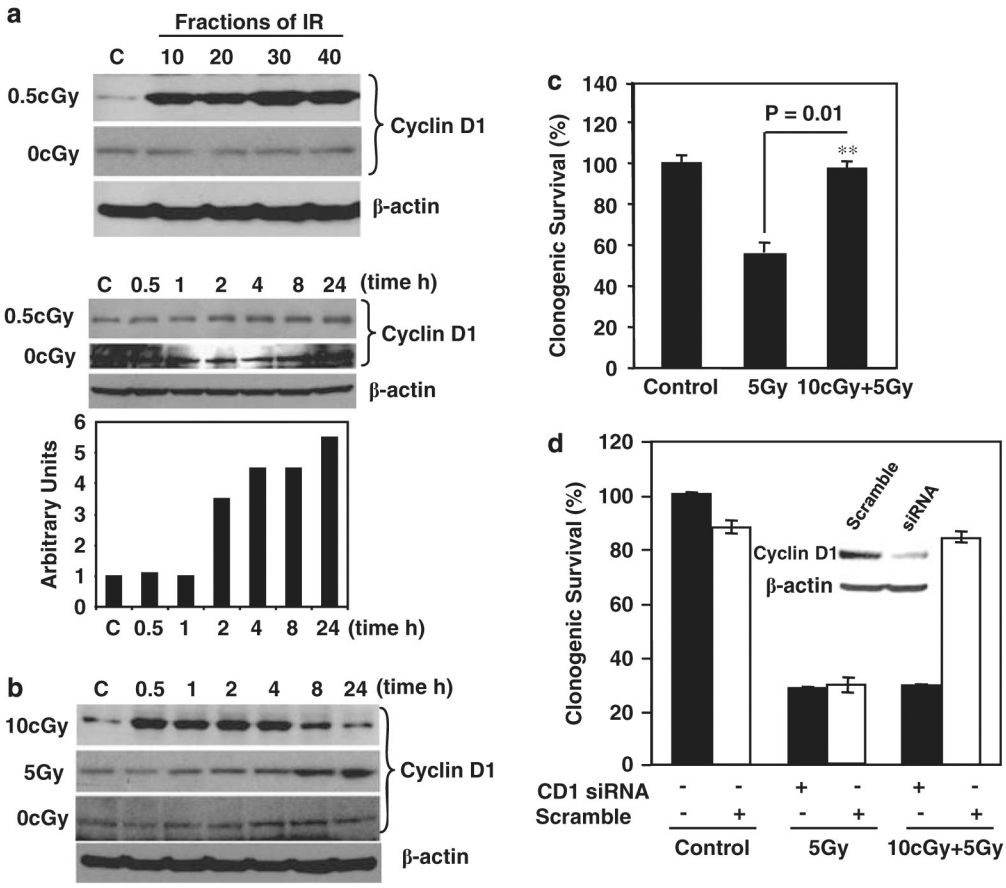

Figure 1.

Low-dose ionizing radiation (LDIR)-induced adaptive radioresistance was eliminated by inhibition of cyclin D1. (**a**) Induction of cyclin D1. HK18 cells were irradiated with 0.5-cGy X-ray for 10, 20, 30 or 40 times (total accumulated doses were 5, 10, 15 or 20-cGy; upper panel). Sham-IR cells (0-cGy) were collected at the same fractions as irradiated cells. Western blot was performed with cellular proteins prepared at 24 h after the final radiation exposure. Lower panel shows western blot and densitometry of cyclin D1 expression in HK18 cells after exposure to a single dose of 0.5-cGy X-ray (C, sham-IR control; β-actin as loading control used for normalization of cyclin D1 levels). (**b**) Induction of cyclin D1 by 10-cGy and 5-Gy γ-ray. HK18 cells were irradiated with a single dose of 10-cGy X-ray or 5-Gy γ-ray and western blot was performed at indicated times after radiation or sham-IR cells (0-cGy; C, sham-IR control; β-actin as loading control). HK18 cells were left untreated (**c**) or treated with 10 nM of cyclin D1 short interfering RNA (siRNA) or scramble (**d**) for 60 h before irradiation with 10-cGy X-ray, and 6 h later a group of dishes were further exposed to 5-Gy γ-ray. Clonogenic survival was measured at 24 h after radiation. Colonies consisting of more than 50 cells were scored as surviving colonies and normalized with the clone numbers observed on nonirradiated cells ($n = 3$). The inset of (**d**) shows a western blot of cyclin D1 and β-actin in cells treated with cyclin D1 siRNA or scramble siRNA.

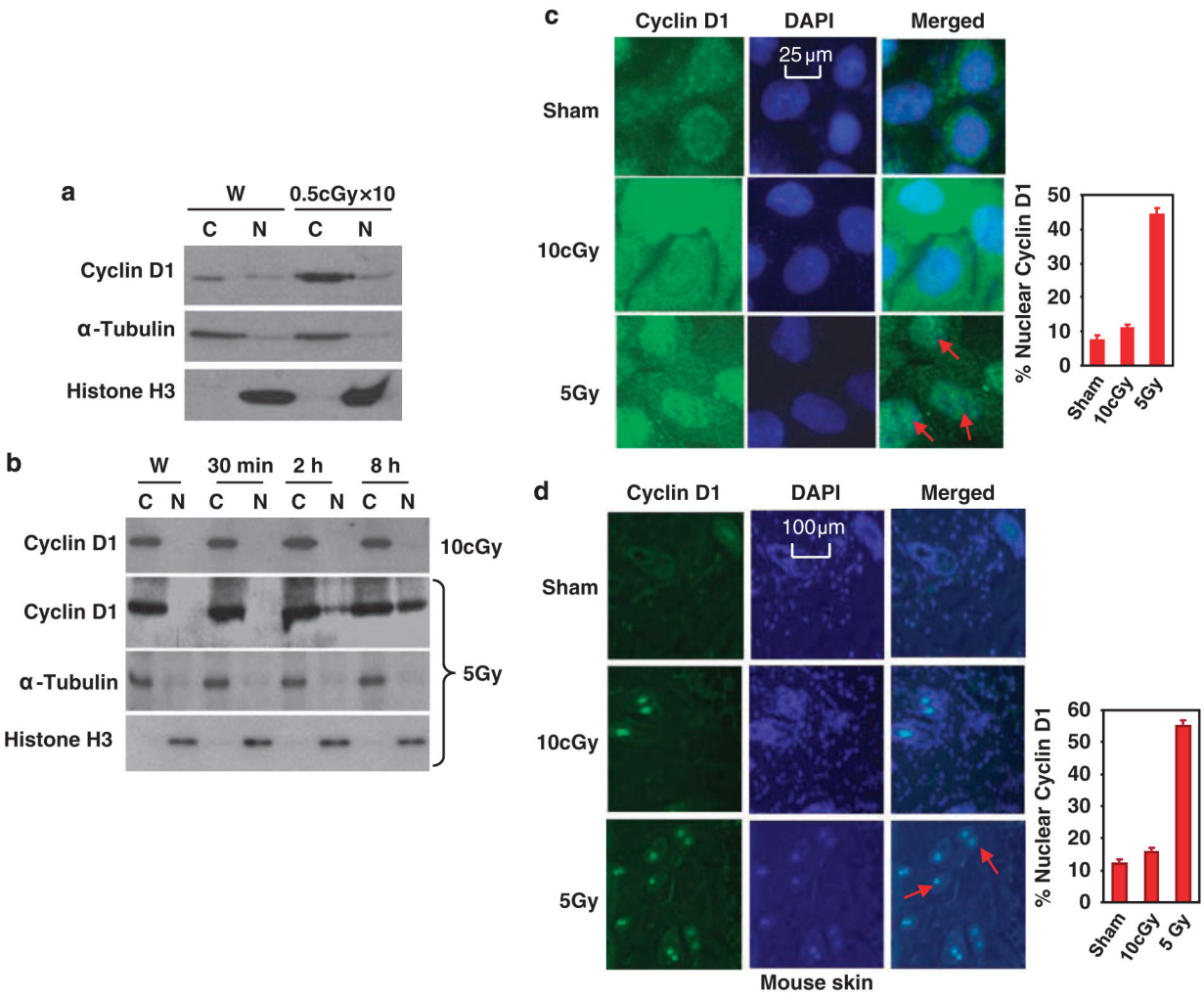

Figure 2.

Differential distribution of cyclin D1 induced by 10-cGy X-ray and 5-Gy γ-ray. (**a**) Cytoplasmic (C) and nuclear (N) proteins were prepared from HK18 cells at 24h after last exposure to 10 fractions of 0.5-cGy X-ray and protein levels were measured with western blotting with α-tubulin and histone H3 as cytoplasmic and nuclear markers (W, sham-LDIR (low-dose ionizing radiation) control). (**b**) Western blotting of cyclin D1 with cytoplasmic (C) and nuclear (N) proteins prepared at indicated time points from HK18 cells after radiation with a low- or high-dose of radiation (α-tubulin and histone H3 as markers for cytoplasmic and nuclear fractions; W, sham-LDIR control). HK18 cells were treated with sham, 10-cGy X-ray or 5-Gy γ-ray, and subjected to immunostaining of cyclin D1 and 4,6-diamidino-2-phenylindole (DAPI) staining of DNA at 8h after radiation (**c**). Skin tissue sections prepared from mice whole-body-irradiated with sham, 10-cGy X-ray or 5-Gy γ-ray were subjected to immunostaining (**d**). Right panels indicate the percentage of cells with nuclear staining of cyclin D1 (100 cells per field were counted and the average of five fields was used to generate the graph).

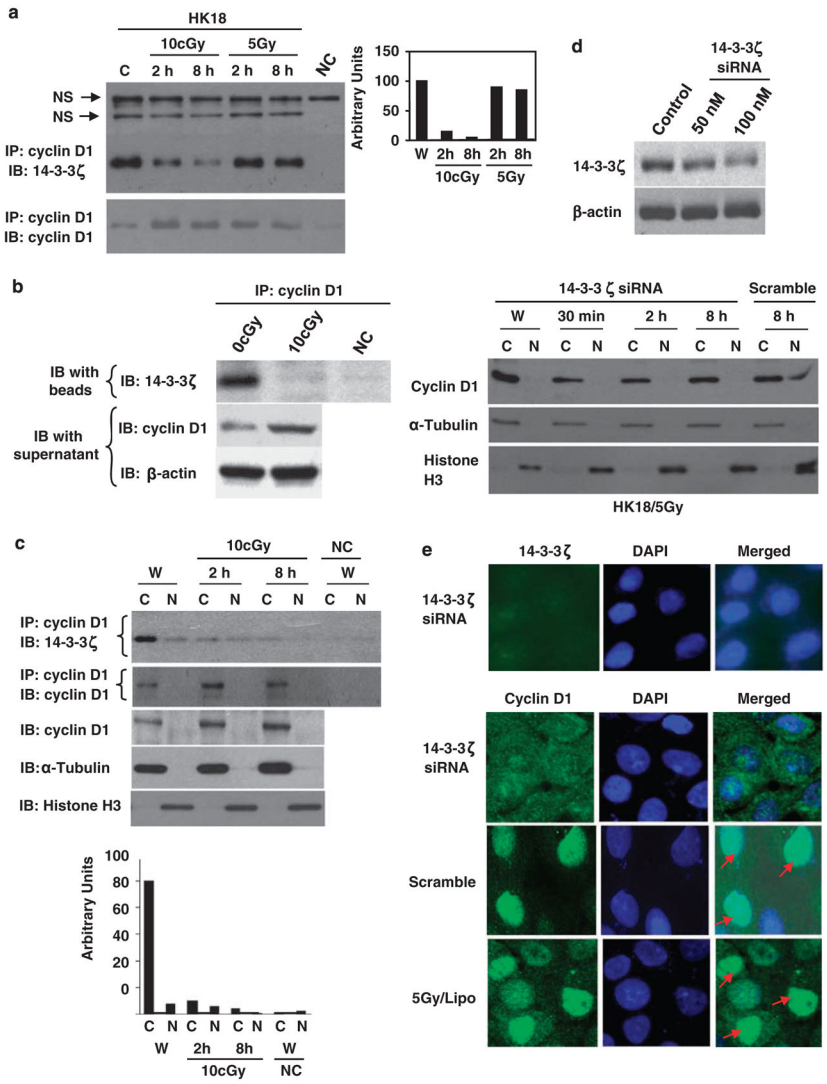

Figure 3.

Cyclin D1 and 14-3-3ζ formed a complex that was dissociated by low-dose ionizing radiation (LDIR). (**a**) Detection of cyclin D1/14-3-3ζ complex. Whole-cell lysates of resting and irradiated HK18 cells were immunoprecipitated with anti-cyclin D1 antibody followed by immunoblotting (IB) with 14-3-3ζ or cyclin D1 antibody. Immunoprecipitation (IP) and IB without cell extracts were included as negative control (NC; right panel, cyclin D1/14-3-3ζ interaction estimated by densitometry). (**b**) Cyclin D1/14-3-3ζ complex dissociation. The upper panel (IP) shows cyclin D1/14-3-3ζ interaction and the lower panel (IB) shows the increased free cyclin D1 in the supernatant (β-actin served as loading control) 8h after LDIR treatment. (**c**) Dissociation of cyclin D1/14-3-3ζ in cytoplasm. Upper panel, cyclin D1/14-3-3ζ interaction was detected in cytoplasmic (C) and nuclear (N) extracts by IP. Extracts of sham-IR cells were preincubated with cyclin D1 antibody included as NC (W, sham-LDIR). Lower panel, western blotting of cyclin D1 (α-tubulin and histone H3 as cytoplasmic and nuclear markers) and the densitometry estimated cyclin D1/14-3-3ζ complex shown in the upper panel. (**d**) Inhibition of 14-3-3ζ by short interfering

RNA (siRNA). Upper panel, western blot of 14-3-3ζ in HK18 cells after transfection with 14-3-3ζ (50 or 100 nM) or scramble siRNA (control; 100 nM) for 60 h. Lower panel, HK18 cells were treated with 100 nM 14-3-3ζ or scramble siRNA before 5-Gy radiation. Cytoplasmic and nuclear cyclin D1 were detected by western blotting. (**e**) Upper panel, HK18 cells transfected with 14-3-3ζ siRNA for 60 h were subjected to immunohistochemistry (IHC) of 14-3-3ζ 8 h after 5-Gy radiation (nucleus visualized by 4,6-diamidino-2-phenylindole (DAPI)). Lower panel, HK18 cells treated with 14-3-3ζ siRNA, scramble or transfection agent (Lipo), and cyclin D1 was detected by IHC 8 h after 5-Gy radiation.

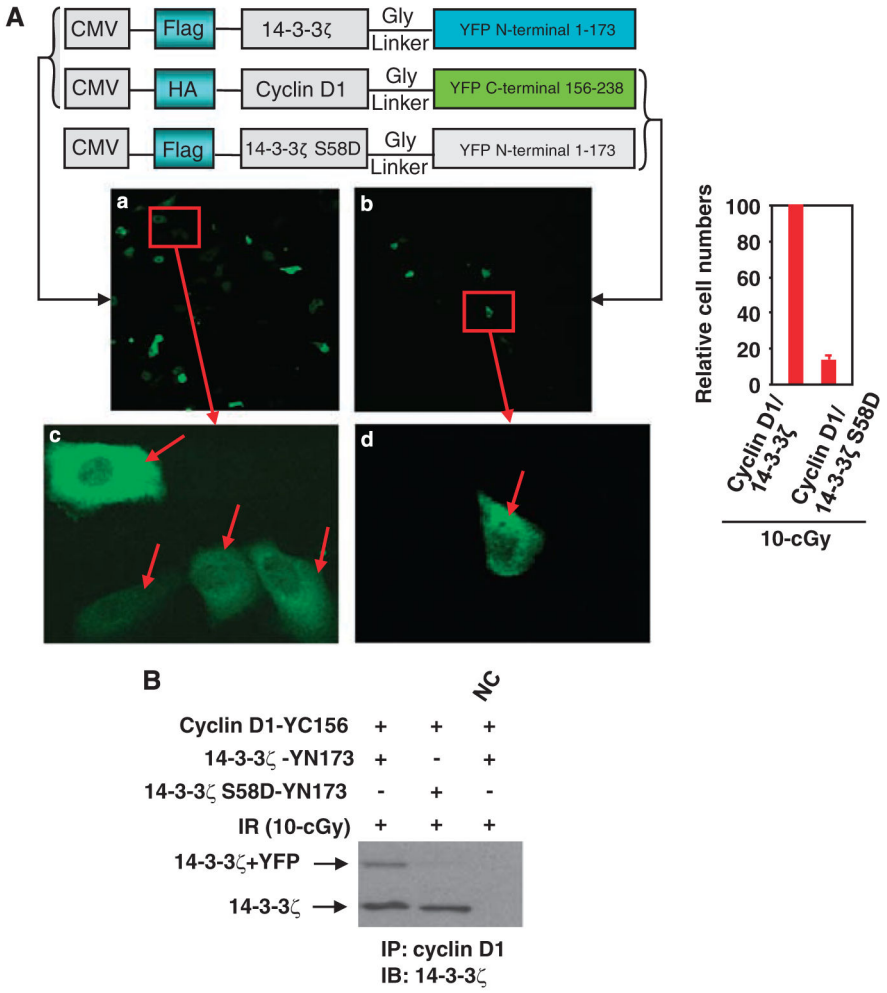

Figure 4.

Ser-58 of 14-3-3ζ was required for cyclin D1 interaction. (**A**) HK18 cells were co-transfected with fusion vectors pFlag-14-3-3ζ-YN173 and pHA-cyclin D1-YC156 or pFlag-14-3-3ζ S58D-YN173 and pHA-cyclin D1-YC156 as indicated. Cells were transfected for 6h and fluorescence images were visualized 24 h after irradiation with 10-cGy. Panels c and d indicate higher magnification of images shown in the red box of a and b, respectively (arrows indicate the formation of 14-3-3ζ/cyclin D1 complex). Right panel shows the estimated difference of cell numbers with fluorescence in panel a versus b. Five fields (100 cells per field) were counted and the average was used to generate the graph. (**B**) Total cell lysates of (**A**) prepared 24h after irradiation with 10-cGy and cyclin D1/14-3-3ζ interaction was detected by IP/IB with indicated antibodies (NC = total cell lysates of HK18 cells of panel A were preincubated with cyclin D1 antibody).

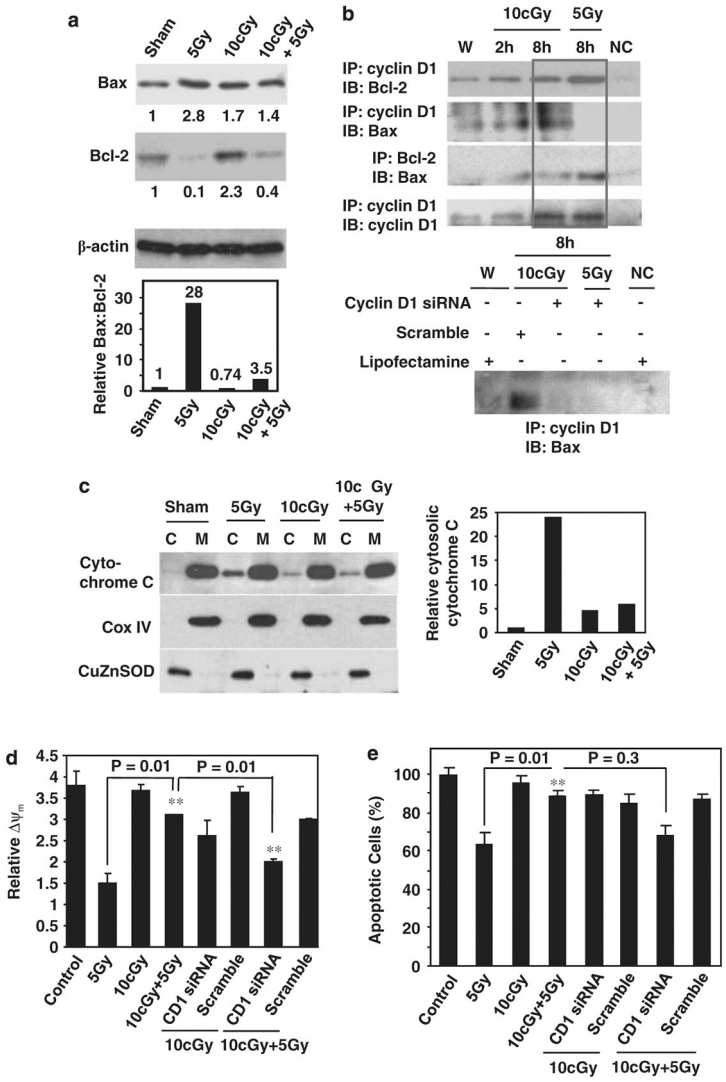

Figure 5.

Cyclin D1/Bax interaction linked with mitochondrial membrane potential ($\Delta\psi_m$) and apoptosis. (**a**) Western blot of Bcl-2 and Bax in HK18 cells treated with sham-IR, 5-Gy, 10-cGy or 10-cGy + 5-Gy IR. Lower panel, the Bax:Bcl-2 ratio determined by relative levels of densitometry. (**b**) IP of whole-cell extracts prepared at indicated times after radiation (W, sham IR). Lower panel, IP and IB were performed with antibodies of cyclin D1 and Bax in HK18 cells treated with 10 nM cyclin D1 or scramble short interfering RNA (siRNA) for 60 h (NC, extracts preincubated with the antibody used for IP; W, sham-IR control). (**c**) Western blotting of mitochondrial and cytosolic cytochrome *c* of HK18 cells treated with as in a (Cox IV and CuZnSOD as markers for mitochondrial and cytosolic fractions; C, cytoplasmic fraction; M, mitochondrial fraction). Right panel shows the relative amount of cytosolic cytochrome *c* estimated by densitometry. (**d** and **e**) Cyclin D1 siRNA inhibited low-dose ionizing radiation (LDIR)-induced $\Delta\psi_m$ and apoptosis. HK18 cells were treated with 10 nM of cyclin D1 siRNA or scramble for 60 h before irradiation as in (**a**). Cells were then treated with JC-1 probe, harvested, and the changes in $\Delta\psi_m$ was measured, using a

fluorescent spectrophotometer (**d**) or stained by terminal deoxynucleotidyltransferase-mediated UTP end labeling (TUNEL) method (**e**) 24h after radiation (mean±s.e., $n = 3$).

Table 1

Cell cycle distribution of HK18 cells after irradiation with 10-cGy and 10-cGy+2-Gy[a]

Radiation	Cell phase		
	G0/G1	S phase	G2/M
Sham-IR	46.66	36.97	16.37
10-cGy	48.91	37.18	13.92
2-Gy	48.98	34.09	16.94
10-cGy + 2-Gy	47.19	36.35	16.46

[a]Values represent the percentage of cells in each phase of the cell cycle.